PHYSICAL REVIEW C, VOLUME 60, 011301

Proton emitters ^{140}Ho and ^{141}Ho: Probing the structure of unbound Nilsson orbitals

K. Rykaczewski,[1,2] J. C. Batchelder,[3] C. R. Bingham,[1,4] T. Davinson,[5] T. N. Ginter,[6] C. J. Gross,[1,3] R. Grzywacz,[2,4] M. Karny,[2,7] B. D. MacDonald,[8] J. F. Mas,[7] J. W. McConnell,[1] A. Piechaczek,[9] R. C. Slinger,[5] K. S. Toth,[1] W. B. Walters,[10] P. J. Woods,[5] E. F. Zganjar,[9] B. Barmore,[4,7] L. Gr. Ixaru,[11] A. T. Kruppa,[7,12] W. Nazarewicz,[1,2,4] M. Rizea,[11] and T. Vertse[7,12]

[1]*Physics Division, Oak Ridge National Laboratory, Oak Ridge, Tennessee 37831*
[2]*Warsaw University, Faculty of Physics, PL-00681 Warsaw, Poland*
[3]*Oak Ridge Institute of Science and Education, Oak Ridge, Tennessee 37831*
[4]*University of Tennessee, Knoxville, Tennessee 37996*
[5]*University of Edinburgh, Edinburgh, EH9 3JZ, United Kingdom*
[6]*Vanderbilt University, Nashville, Tennessee 37235*
[7]*Joint Institute for Heavy Ion Research, Oak Ridge, Tennessee 37831*
[8]*Georgia Institute of Technology, Atlanta, Georgia 30332*
[9]*Louisiana State University, Baton Rouge, Louisiana 70803*
[10]*University of Maryland, College Park, Maryland 20742*
[11]*Institute of Physics and Nuclear Engineering ''Horia Hulubei,'' P.O. Box MG-6, Bucharest, Romania*
[12]*Institute of Nuclear Research, Hungarian Academy of Sciences, H-4001 Debrecen, Hungary*

(Received 24 February 1999; published 16 June 1999)

Two new proton emitting states in the deformed nuclei ^{140}Ho ($E_p = 1086 \pm 10$ keV, $T_{1/2} = 6 \pm 3$ ms) and ^{141m}Ho ($E_p = 1230 \pm 20$ keV, $T_{1/2} = 8 \pm 3$ μs) have been identified. Experimental data are interpreted using the coupled-channels Schrödinger equation with outgoing wave boundary conditions. The observed resonances are discussed in terms of deformed single-proton orbitals close to the $Z = 67$ Fermi level. [S0556-2813(99)50107-6]

PACS number(s): 23.50.+z, 21.10.Tg, 24.10.Eq, 27.60.+j

Proton radioactivity is an excellent example of elementary three-dimensional quantum-mechanical tunneling. The lifetimes of proton emitters provide very direct information on wave functions of the narrow proton resonances, while the energies of emitted protons tell us about nuclear binding energies in the vicinity of the proton drip line.

Including the radioactivities of ^{140}Ho and ^{141m}Ho presented here, as many as 23 ground-state proton emitters and 12 proton-decaying excited states have been found [1–7]. For most of those states, proton emission rates can be well understood within a spherical picture [8] in which a single proton tunnels through the Coulomb-plus-centrifugal barrier. However, it was long recognized that in some cases, such as ^{109}I [9–11] and ^{113}Cs [9,12–14], deformation effects can play a role [15,16].

A new avenue in the spectroscopy of proton emitters has opened up with the discovery of the ground-state proton radioactivity of ^{131}Eu and ^{141}Ho [5]. Unlike the cases of ^{109}I and ^{113}Cs, the associated quadrupole deformations are large, $\beta_2 > 0.2$. In Ref. [5], proton half-lives were computed within the distorted-wave Born approximation (DWBA) approach [15,16] and the data were interpreted in terms of the $7/2^-[523]$ state in ^{141}Ho, and the $3/2^+[411]$ and $5/2^+[413]$ Nilsson orbitals in ^{131}Eu.

The objective of this work is twofold. The first goal is to extend the studies of proton radioactivity among highly deformed nuclei. With a $(p,5n)$ reaction channel used for the first time in such studies, this work is probing the experimental observation limits for detecting proton emitters produced in a fusion-evaporation reaction and studied by means of a recoil mass separator (RMS) [17] coupled to a double-sided silicon strip detector (DSSD) [18]. Secondly, we apply the recently developed theoretical formalism based on the coupled-channels Schrödinger equation with outgoing wave boundary conditions to the observed deformed narrow resonances. As shown below, theory gives a robust prediction concerning the nature of the observed states.

A 0.91 mg/cm^2 thick target of isotopically enriched ^{92}Mo was bombarded with 315-MeV ^{54}Fe ions accelerated at the Holifield Radioactive Ion Beam Facility (HRIBF) at Oak Ridge, with an average beam current on target of ~ 13 particle nA during a period of 30 hours. Fusion-evaporation products of interest, recoiling with an energy of 97 ± 10 MeV, passed through the RMS and a gas-filled position-sensitive avalanche counter (PSAC) for mass and charge identification [17], and then were slowed down by a 1.17 mg/cm^2 nickel foil before implantation into a 60-μm thick DSSD. The DSSD had an active area of 4 cm $\times 4$ cm with a total of 40 horizontal and 40 vertical strips, providing 1600 individual pixels of 1 mm^2 each. The RMS was adjusted to deposit the $A = 140$ and a part of the $A = 141$ products having a charge state $+27$ on the DSSD, see Fig. 1. For each implant, the energy of the implant, the pixel in which the implant occurred, the PSAC information, and the time were recorded. If a decay occurred within a time of 240 μs after an implant, the decay energy, pixel number, and time of decay were also recorded in the same event. For decay times greater than 240 μs, the decay information was recorded as a separate event. Decays within a given pixel were correlated with the previous implants in the same pixel in order to determine the decay time of the radioactivity.

Figure 2 shows the low-energy spectrum of charged par-

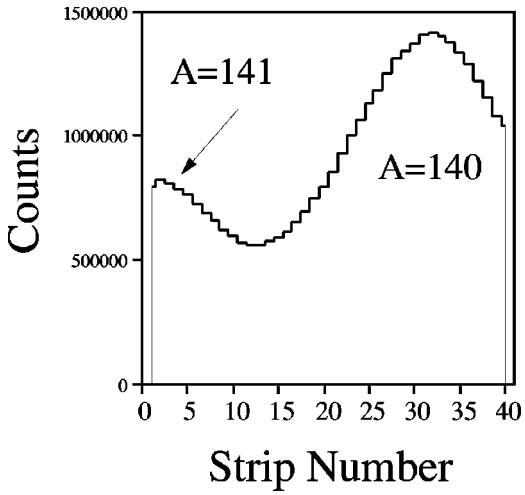

FIG. 1. DSSD mass spectrum of $A=140$ and $A=141$ recoils obtained during the described experiment. The mass gates corresponding to DSSD vertical strip numbers were used to distinguish between ^{141}Ho and ^{140}Ho proton decays. For the latter gate, the signals from strips 24 through 37 were taken.

ticles recorded in the DSSD within the given time intervals Δt after recoil implantation. The respective $A=141$ and $A=140$ mass gates were applied, cf. Fig. 1. A peak of about 100 counts in the middle panel of Fig. 2, obtained for $\Delta t \leqslant 25$ ms and $A=141$, is that of the known proton decay [5] of the ^{141}Ho ground state. Its energy, reported in Ref. [5] as 1169 ± 8 keV, was taken together with the well-known proton lines of ^{109}I, ^{113}Cs, and ^{147}Tm [2,3] to calibrate the DSSD energy spectra. The half-life of $^{141g.s.}$Ho was remeasured to be 3.9 ± 0.5 ms, in good agreement with 4.2 ± 0.4 ms given in Ref. [5]. By keeping the same $A=141$ mass gate and reducing the recoil-decay correlation time Δt to 200 μs, a peak of about 10 counts at 1230 ± 20 keV was found, see upper panel of Fig. 2. The 20 keV error bar for the peak energy value, larger than a purely statistical one, accounts for an energy shift due to the amplifier overload effects for short correlation times Δt—see the detailed discussions in our previous papers reporting short-lived proton emitters ^{145}Tm ($T_{1/2}=3.5$ μs [4]) and ^{151m}Lu ($T_{1/2}=16$ μs [7]). The time distribution of the events displayed in the upper panel of Fig. 2 corresponds to a half-life of 8 ± 3 μs. The conditions $\Delta t \leqslant 25$ ms and mass gate $A=140$ applied to the same experimental data reveal two peaks, one of them at 1.17 MeV coming from a tail of the $A=141$ mass distribution (cf. Fig. 1), and a new one at 1086 ± 10 keV with a decay pattern corresponding to a $T_{1/2}$ of 6 ± 3 ms. Since the energies of the latter 11 events are obtained with relatively long recoil-decay correlation times, and thus are not modified by the amplifier overload effect, the peak energy can be given within a 10 keV error bar.

These counting rates correspond to the cross section σ of ≈130 nb for $^{141g.s.}$Ho and ≈30 nb for the new activity observed at mass $A=141$. The cross section for the new $A=140$ proton radioactivity is about 13 nb. The σ values assume 3% transmission efficiency for the RMS. All of the $A=140$ and $A=141$ isobars, other than holmium isotopes,

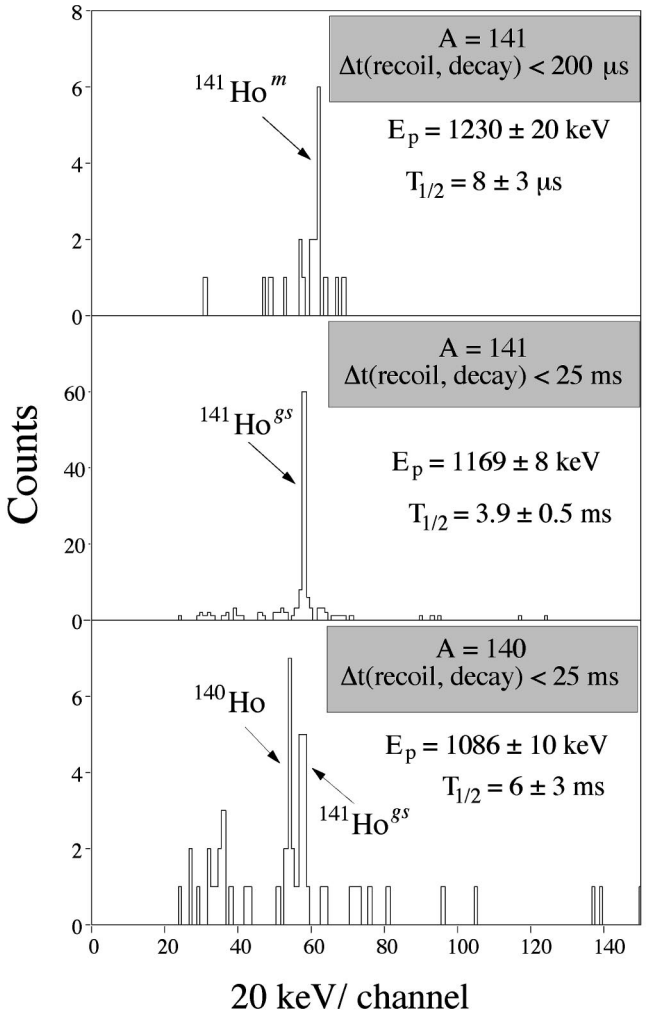

FIG. 2. The low-energy particle spectra observed during the HRIBF experiment. The correlation times Δt and mass gates used for each graph are indicated.

produced in the ^{54}Fe+^{92}Mo fusion-evaporation reaction are either stable against proton emission [19,20], or have negligible production cross sections (such as ^{140}Er, produced in $6n$ evaporation channel, which is below 1 pb level). Therefore, we assign the new radioactivities to ^{140}Ho and ^{141m}Ho, respectively. The predicted [21] cross sections for ^{141}Ho and ^{140}Ho averaged over the ^{92}Mo target thickness are about 300 nb and 50 nb, respectively, a factor of 2 to 4 larger than measured. However, since the extrapolated mass values are used for the HIVAP cross-section calculations [21] and the assumed RMS transmission of 3% is somewhat uncertain, we consider such a discrepancy as small.

The single-quasiproton bandheads of rare-earth nuclei have been analyzed in Ref. [22]. Here, we have extended these calculations to proton-rich holmium isotopes. For ^{151}Ho, ^{149}Ho and ^{147}Ho, the equilibrium shape is spherical due to the proximity of the $N=82$ shell closure, and all these isotopes have $h_{11/2}$ ground states. While ^{145}Ho is a weakly deformed transitional system, the lighter isotopes, ^{143}Ho and ^{141}Ho, are predicted to be highly deformed. The calculated equilibrium deformations for the low-lying one-quasiparticle

states of ^{141}Ho are very similar: $\beta_2 \approx 0.27$ and $\beta_4 \approx -0.07$ (similar deformations were also obtained in Ref. [20]). The predicted ground state of ^{141}Ho is the $1/2^+[411]$ Nilsson level and the lowest excited states are the $7/2^-[523]$ and $5/2^-[532]$ ($h_{11/2}$) orbitals. Still higher in energy lies a $5/2^+[413]$ and $3/2^+[411]$ pseudospin doublet.

Thanks to the large equilibrium deformation, we can assume that the wave function of the odd-Z parent nucleus (here: ^{141}Ho) is that of the particle-plus-rotor model in the strong coupling limit [15]. Furthermore, we assume that the daughter even-even nucleus is in its ground state. Consequently, the angular momentum carried by the emitted proton is $j_p = \Omega$, where Ω is the projection of the total single particle angular momentum onto the symmetry axis.

The width of the deformed proton resonance can be written as [15] $\Gamma = S_p \Gamma_{\text{s.p.}}$, where S_p is the proton spectroscopic factor and $\Gamma_{\text{s.p.}}$ is the width of the deformed single-particle resonance representing the tunneling through the deformed Coulomb barrier. Our approach for calculating $\Gamma_{\text{s.p.}}$ is similar to that described in Refs. [23,24] but significantly differs in details [25] and interpretation [26]. The wave function of a single particle in a bound or quasibound state characterized by definite values of parity π and Ω can be expanded into a sum of partial waves

$$\psi_{\Omega\pi}(\boldsymbol{r}) = \sum_{l,j} \frac{u_{lj}^{\Omega\pi}(r)}{r} [Y_l(\hat{r})\chi_{1/2}]_{j\Omega}. \quad (1)$$

The radial wave functions $u_{l,j}^{\Omega\pi}(r)$ satisfy a system of coupled equations

$$\left[\frac{d^2}{dr^2} - \frac{l_\alpha(l_\alpha+1)}{r^2} - k^2\right] u_\alpha^{\Omega\pi}(r) = \sum_{\alpha'} v_{\alpha'\alpha}^{\Omega\pi} \; u_{\alpha'}^{\Omega\pi}(r) \quad (2)$$

for each $\alpha = [l,j]$ channel which can be coupled for the given Ω and parity considered. Here k denotes the wave number ($k^2 = 2\mu/\hbar^2 \varepsilon$; μ is the reduced mass and ε is the single-particle energy) and $v_{\alpha'\alpha}^{\Omega\pi}$ is the coupling potential between channels α and α'. Each radial component in Eq. (2) should be regular in the origin and should be proportional to a purely outgoing Coulomb wave in the asymptotic region. These boundary conditions can be satisfied only at certain discrete complex values of the wave number k, i.e., at the bound and resonant eigenvalues. For resonant states, the single-particle energy ε becomes complex, i.e., $\varepsilon = \varepsilon_0 - i/2\Gamma_{\text{s.p.}}$. Normalization of the resonant wave functions can be done with different regularization methods. Here we applied the ''exterior complex scaling'' method [27] which has been used also in the program GAMOW describing spherical geometry [28]. For integrating the coupled equations numerically we used the code CCGAMOW which applies the piecewise perturbation method [29] generalized to the coupled-channels case. The details of the numerical procedure are given in Ref. [25].

In our calculations, the proton optical potential was approximated by an average Woods-Saxon (WS) field, containing the central term and the spin-orbit potential. The radius and diffuseness of the optical potential were taken from Ref. [30]; this parametrization turned out to work very well in the description of spherical proton emitters [8]. The uncertainty in the proton-nucleus optical model potential does not make it possible to *predict* positions of one-quasiparticle states in the parent nucleus with an accuracy better than a few hundred keV [22]. Consequently, following Ref. [8], the depth of the central potential V_0 was adjusted for each orbital to reproduce the experimental Q_p value (which slightly differs from E_p due to the presence of recoil and screening corrections [2]). For the depth of the spin-orbit potential, we adopted a simple ansatz $V_{0,\text{so}} = \kappa \cdot V_0$. The factor κ was adjusted to reproduce the order of spherical single-proton orbitals in the rare earth region ($50 < Z < 82$), and the optimal (and adopted) value turned out to be $\kappa = -0.26$. The deformed WS potential was defined as in Ref. [31] and its multipole decomposition was carried out numerically assuming $\lambda_{\max} = 12$. In the partial-wave expansion of Eq. (1) all partial waves with $l \leqslant 17$ were considered. In our calculations, we ignored the contribution to the coupling potential coming from the nonspherical part of the spin-orbit term. According to the discussion in Ref. [32], the influence of the deformation-dependent part of the spin-orbit potential on the single-particle orbitals is very weak. Also, variations in the spin-orbit potential have a negligible effect on the tunneling rate [8]. The spectroscopic factors S_p have been estimated in the independent-quasiparticle picture, assuming the strong coupling approximation [15]: $S_p = u_\Omega^2/(\Omega + 1/2)$.

Since the resonance widths can be as small as 10^{-22} MeV, an unprecedented numerical accuracy is required. Our calculations were done with the extended precision arithmetic, and the resulting value of $\Gamma_{\text{s.p.}}$ was compared with that obtained from the continuity relation (9.12) of Ref. [33]. In all cases excellent agreement was obtained. (As stated in Ref. [26], this way of calculating $\Gamma_{\text{s.p.}}$ is more consistent than the R-matrix expression applied in Ref. [24]; see also the discussion in [34].)

Figure 3 displays the calculated half-lives of the $1/2^+[411]$, $7/2^-[523]$, $5/2^-[532]$, and $5/2^+[413]$ resonances as a function of quadrupole deformation β_2 ($\beta_4 = -0.06$). It shows that in the considered region of β_2, the half-lives depend very weakly on deformation. (We have also checked that the half-lives are practically independent on β_4 in the range $-0.08 < \beta_4 < -0.04$.) The fact that the predicted widths only vary weakly with deformation around $\beta_2 = 0.27$ allows for robust theoretical predictions regarding the nature of resonances in ^{141}Ho.

The 4 ms state at $Q_p = 1.19$ MeV (most likely the ground state of ^{141}Ho) can be associated with the $7/2^-[523]$ orbital which yields $T_{1/2} \approx 8$ ms. In heavier deformed Ho isotopes with $N > 82$ the ground state is clearly a $7/2^-[523]$ level. The $5/2^-[532]$ Nilsson state is predicted to have a very similar half-life; it is calculated to be a hole state with a rather small spectroscopic factor ($u^2 \approx 0.23$). Since there is much uncertainty regarding the position of Nilsson orbitals in the deformed rare-earth nuclei with $N < 82$, the $5/2^-[532]$ assignment cannot be excluded although it seems less likely. (In any case, the $7/2^-[523]$ and $5/2^-[532]$ orbitals should be mixed by the Coriolis interaction, neglected in this work

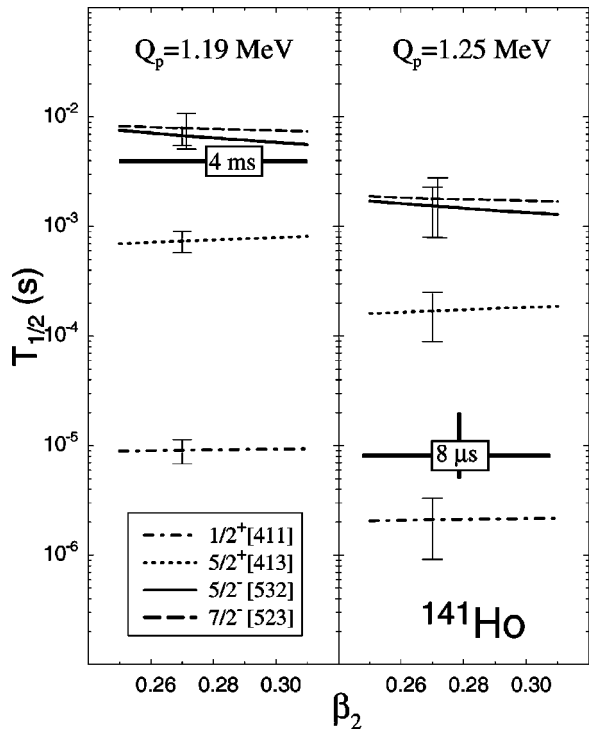

FIG. 3. Calculated half-lives for the $1/2^+[411]$, $7/2^-[523]$, $5/2^-[532]$, and $5/2^+[413]$ resonances as functions of quadrupole deformation β_2 ($\beta_4=-0.06$) assuming $Q_p=1.19$ MeV (left) and 1.25 MeV (right). The experimental half-lives are indicated by thick lines. The errors in calculated half-lives come from an uncertainty in the experimental Q_p.

[22].) Davids *et al.* [5] assigned the ^{141gs}Ho to the $7/2^-[523]$ state, and a similar conclusion was drawn in [24].

The only candidate for an 8 μs resonance at $Q_p=1.25$ MeV is the $1/2^+[411]$ Nilsson level. Indeed, it is the only orbital with a half-life in the μs range. For comparison, we also performed calculations for the $5/2^+[413]$ level which is expected to lie higher in energy. Its half-life, $T_{1/2}\approx 0.1$ ms, is not consistent with the present data. Maglione *et al.* [24] also conclude that the $1/2^+$ level is the only plausible candidate.

In the absence of interference effects due to level crossings (see, e.g., Ref. [24] for an illustrative example) the particle decay width of a deformed Nilsson orbital is governed by the partial wave with the lowest value of angular momentum allowed. Table I shows the partial widths $\gamma_{lj}\equiv\Gamma_{lj}/\Gamma_{\text{s.p.}}$, together with the probabilities $|c_{lj}|^2$ that a partial wave (lj) appears in the expansion (1). As expected, proton decay is almost completely governed by the lowest-l wave appearing in the deformed wave function, i.e., the f wave for the $7/2^-[523]$ and $5/2^-[532]$ orbitals, the d wave for the $5/2^+[413]$, and the s wave for the $1/2^+[411]$ level. In this context, it is interesting to note that for a spherical resonance at $Q_p=1.19$ MeV the calculated half-life is ~ 30 ms for $l=5$ and ~ 0.1 ms for $l=3$. Hence, the calculated half-life of ~ 8 ms of the deformed resonance comes as a result of an interplay between the large penetrability of the f wave through the deformed barrier, and the large content of an h wave in the wave function (86%). The low-l components that are not present in the spherical shape appear at large deformations thanks to the multipole coupling. Table I shows that even a small admixture of a low-l partial wave ($|c_{lj}|^2\sim 10\%$) is sufficient to completely determine the decay process ($\gamma_{lj}\sim 1$).

TABLE I. Partial widths γ_{lj} and spherical amplitudes $|c_{lj}|^2$ for the deformed resonances in ^{141}Ho ($\beta_2=0.27$, $\beta_4=-0.06$) calculated with $Q_p=1.19$ MeV. Only components with γ_{lj} or $|c_{lj}|^2$ greater than 4% are shown.

Orbital	l_j	γ_{lj}	$\lvert c_{lj}\rvert^2$
$1/2^+[411]$	$s_{1/2}$	0.77	0.18
	$d_{3/2}$	0.16	0.24
	$d_{5/2}$	0.07	0.18
	$g_{7/2}$	~ 0	0.34
$5/2^+[413]$	$d_{5/2}$	0.96	0.17
	$g_{7/2}$	0.04	0.75
$5/2^-[532]$	$f_{7/2}$	0.94	0.14
	$h_{11/2}$	0.03	0.81
$7/2^-[523]$	$f_{7/2}$	0.91	0.08
	$h_{11/2}$	0.08	0.86

The structure of the odd-odd nucleus ^{140}Ho is more complex. Since the half-life of ^{140}Ho is in the millisecond range, it is reasonable to assume, with an analogy to the decay of ^{141gs}Ho, that the odd proton in ^{140}Ho occupies the $7/2^-[523]$ orbital. The neutron single-quasiparticle states predicted to be close to the Fermi surface are $5/2^+[402]$ and $9/2^-[514]$ states originating from the $d_{5/2}$ and $h_{11/2}$ shells, respectively. According to our calculations, both states, the $\pi(7/2^-[523])\otimes\nu(5/2^+[402])$ and $\pi(7/2^-[523])\otimes\nu(9/2^-[514])$ are close in energy and are candidates for the ground-state configuration of ^{140}Ho. The structure of the ^{140}Ho wave function is affected by the residual proton-neutron interaction between the valence nucleons (perhaps causing a somewhat shorter half-life). The theoretical analysis of the resulting configuration mixing and its impact on the proton decay width will be the subject of a forthcoming study.

Additional information gained from our study is related to the energy surface of proton drip line nuclei. The energy of the proton line from odd-odd ^{140}Ho decay is lower than the one from neighboring odd-even ^{141}Ho. Such a pattern was already noticed [13] for the nuclei in the transitional region above $Z=50$. For spherical proton emitters with $Z\geqslant 69$ this energy dependence is reversed, with the Q_p always increasing when departing from the β-stability line, see, e.g., [3]. An observation of a proton line from ^{140}Ho at almost 100 keV below the one in ^{141}Ho may explain the nonobservation of a proton decay of ^{136}Tb and ^{137}Tb in a 35 hour experiment with a 15 particle nA, 290 MeV ^{50}Cr beam on a 0.91 mg/cm^2 ^{92}Mo target. While the various mass predictions, see, e.g., Ref. [19], point to proton energies well below 1 MeV for ^{137}Tb, the nucleus ^{136}Tb is calculated to be more proton unstable. However, our result for the ^{140}Ho - ^{141}Ho pair might indicate an opposite pattern.

In summary, the evidence for the deformed Nilsson proton resonances has been found in ^{141}Ho and ^{140}Ho. The data were interpreted using the coupled-channels method with the deformed optical potential. The excited state in ^{141}Ho discovered in this work has been interpreted in terms of the $1/2^+[411]$ level, and its ground state is the $7/2^-[523]$ orbital, although the Coriolis coupling with other levels originating from the $h_{11/2}$ shell cannot be excluded. It is concluded that the decay process of a deformed resonance is primarily governed by the lowest-l partial wave allowed by angular momentum and parity conservation (see also Ref. [35]). An obvious extension of the present theoretical approach is to take into account the effects of the Coriolis coupling. This will make it possible to consistently describe the interplay between γ emission and proton decay from deformed nuclei.

ORNL is managed by LMER Corporation under Contract No. DE-AC05-96OR22464 with the U.S. DOE. This work was supported by the U.S. DOE through Contract Nos. DE-FG02-96ER40983 and DE-FG02-96ER40963 (UT), DE-AC05-76OR00033 (ORISE), DE-FG05-88ER40407 (Vanderbilt), DE-FG02-96ER40978 (LSU), and DE-FG05-88ER40330 (Georgia Tech). JIHIR has as member institutions the UT, Vanderbilt, and ORNL; it is also supported by the U.S. DOE. This work was partially supported by the Polish KBN (MK), the Soros Foundation, Hungary (ATK), and the Hungarian NRF OTKA through Contract No. T26244 (TV).

[1] K. P. Jackson *et al.*, Phys. Lett. **33B**, 281 (1970).
[2] S. Hofmann, Radiochim. Acta **70/71**, 93 (1995).
[3] P. J. Woods and C. N. Davids, Annu. Rev. Nucl. Part. Sci. **47**, 541 (1997).
[4] J. C. Batchelder *et al.*, Phys. Rev. C **57**, R1042 (1998).
[5] C. N. Davids *et al.*, Phys. Rev. Lett. **80**, 1849 (1998).
[6] J. Uusitalo *et al.*, in *ENAM98: Exotic Nuclei and Atomic Masses*, AIP Conf. Proc. No. 455, edited by B. M. Sherrill, D. J. Morrisey, and C. N. Davids (AIP, New York, 1998), p. 375.
[7] C. R. Bingham *et al.*, Phys. Rev. C **59**, R2984 (1999).
[8] S. Åberg, P. B. Semmes, and W. Nazarewicz, Phys. Rev. C **56**, 1762 (1997); **58**, 3011 (1998).
[9] T. Faestermann *et al.*, Phys. Lett. **137B**, 23 (1984).
[10] F. Heine *et al.*, Z. Phys. A **340**, 23 (1984).
[11] P. J. Sellin *et al.*, Phys. Rev. C **47**, 1933 (1993).
[12] A. Gillitzer *et al.*, Z. Phys. A **326**, 107 (1987).
[13] R. D. Page *et al.*, Phys. Rev. Lett. **72**, 1798 (1994).
[14] C. J. Gross *et al.*, in *ENAM98: Exotic Nuclei and Atomic Masses* [6], p. 444.
[15] V. P. Bugrov and S. G. Kadmensky, Sov. J. Nucl. Phys. **49**, 967 (1989).
[16] S. G. Kadmensky and V. P. Bugrov, Phys. At. Nucl. **59**, 399 (1996).
[17] C. J. Gross *et al.*, in *Application of Accelerators in Research and Industry*, AIP Conf. Proc. 392 (AIP, New York, 1997), p. 401.
[18] P. J. Sellin *et al.*, Nucl. Instrum. Methods Phys. Res. A **311**, 217 (1992).
[19] P. E. Haustein (ed.), At. Data Nucl. Data Tables **39**, 185 (1988).
[20] P. Möller, J. R. Nix, W. D. Myers, and W. J. Swiatecki, At. Data Nucl. Data Tables **59**, 185 (1995).
[21] W. Reisdorf, Z. Phys. A **300**, 227 (1981).
[22] W. Nazarewicz, M. A. Riley, and J. D. Garrett, Nucl. Phys. **A512**, 61 (1990), and references therein.
[23] L. S. Ferreira, E. Maglione, and R. J. Liotta, Phys. Rev. Lett. **78**, 1640 (1997).
[24] E. Maglione, L. S. Ferreira, and R. J. Liotta, Phys. Rev. Lett. **81**, 538 (1998); Phys. Rev. C **59**, R589 (1999).
[25] A. T. Kruppa, T. Vertse, L. Gr. Ixaru, and M. Rizea (in preparation).
[26] A.T. Kruppa *et al.* (unpublished).
[27] B. Gyarmati and T. Vertse, Nucl. Phys. **A160**, 523 (1971).
[28] T. Vertse, K. F. Pál, and Z. Balogh, Comput. Phys. Commun. **27**, 309 (1982).
[29] L. Gr. Ixaru, *Numerical Methods for Differential Equations* (Reidel, Dordrecht, 1984).
[30] F. D. Becchetti, Jr. and G. W. Greenlees, Phys. Rev. **182**, 1190 (1969).
[31] S. Ćwiok, J. Dudek, W. Nazarewicz, J. Skalski, and T. Werner, Comput. Phys. Commun. **46**, 379 (1987).
[32] S. G. Nilsson, Mat. Fys. Medd. K. Dan. Vidensk. Selsk. **29**, 16 (1955).
[33] J. Humblet and L. Rosenfeld, Nucl. Phys. **26**, 529 (1961).
[34] A. Arima and S. Yoshida, Nucl. Phys. **A219**, 475 (1974).
[35] T. Misu, W. Nazarewicz, and S. Åberg, Nucl. Phys. **A614**, 44 (1997).